RSC Advances

PAPER

View Article Online
View Journal | View Issue

Cite this: *RSC Adv.*, 2021, **11**, 1850

Bio-engineered palladium nanoparticles: model for risk assessment study of automotive particulate pollution on macrophage cell lines

Aarzoo,[a] Saba Naqvi,*[b] Nidhi Bharal Agarwal,[c] Manoj P. Singh[d] and M. Samim*[a]

Received 2nd November 2020
Accepted 16th December 2020

DOI: 10.1039/d0ra09336j

rsc.li/rsc-advances

The surge in vehicular activity in densely populated areas has led to an increased concentration of airborne palladium nanoparticles (PdNPs) in the environment. Recent toxicity data have indicated that PdNPs exhibit adverse effects in *in vitro* and *in vivo* models, however, their effect on the immune system is not fully understood. Therefore, in the present study, we aimed to evaluate possible toxic effects of bio-engineered palladium nanoparticles on the murine macrophage cell line (J774). Here we prepared palladium nanoparticles using aqueous leaf extract of *Parthenium hysterophorus* and characterized them by UV-Vis spectroscopy, XRD, FT-IR spectroscopy, HR-TEM, EDX, SEM and zeta potential. Toxicity parameters such as cell viability, cell membrane integrity, induction of apoptosis and ROS production were assessed on J774 cell lines. Spherical palladium nanoparticles of mean size ~4 nm, when subjected to time and dose-dependent cytotoxicity assay, showed cell viability was >95% at lower doses (25, 200 μg mL^{-1}) and <50% at higher doses of palladium nanoparticles (400, 500 μg mL^{-1}) after 24 hours of incubation. We also observed cell membrane injury at higher doses by lactate dehydrogenase assay. The induction of apoptosis observed was moderate. H_2DCFDA assay revealed visible cell damage which could be due to modest levels of ROS generation. The detection of Pd in the road-dust samples of New Delhi using inductively coupled plasma-mass spectroscopy (ICP-MS) technique was also investigated.

1 Introduction

Air pollution is one of the largest environmental health risks, causing around 7 million deaths annually all over the world.[1,2] The steady rise in outdoor air pollution and ambient particulate matter (PM) in the urban environment is mainly found to be linked with increased vehicular activity in densely populated regions.[3,4] As a result, this has shown to have increased morbidity and mortality of respiratory and cardiovascular diseases in individuals, especially, those who work in heavy-traffic regions.[5] Individuals already suffering from conditions such as chronic obstructive pulmonary disease (COPD), asthma or lung cancer are even at higher risk which could also result in their premature death.

The platinum group elements (PGEs) are a group of rare and high-value noble transition metals which are naturally found in a very low concentration in the earth's crust (<1 ng g^{-1}).[6] They are known for their remarkable catalytic properties.[7,8] However, over the years, PGEs, notably, palladium (Pd), platinum (Pt) and rhodium (Rh), have become a matter of environmental concern. Since their introduction in vehicles as a catalyst in three-way catalytic converters from the mid-1970s, a large amount of mass transfer of PGEs due to their mining and increased vehicular activity has led to a disturbance in the biogeochemical cycles with their anthropogenic fluxes exceeding their natural flow in the environment.[9,10] This has resulted in the accumulation of PGEs in the urban environment media such as in soil,[11,12] road-dust,[13,14] vegetation,[15,16] seawater,[17] sewage sludge,[18] aerosols[19] and in aquatic organisms as well as birds.[20,21] PGEs have also been measured in the remotest of areas such as in the snow of Antarctica and Greenland.[22,23]

A three-way catalytic converter (TWC) is fitted in the exhaust system of automobiles which is mainly designed to mitigate noxious pollutants present in the environment by catalysing the conversion of harmful gases (carbon monoxide, nitrogen oxides and hydrocarbons) into benign products usually by reduction or oxidation reaction.[9,24] The surface of the TWC is made up of a honeycomb support design coated with alumina layer also called as washcoat which is activated by adding some metal additives. On the surface of the washcoat, 0.2 weight% of respective PGEs salts with varying proportions are embedded.[25,26] Since the 1990s, Pd metal has largely substituted Pt and Rh in TWCs as it is more cost-effective and more resilient

[a]*Department of Chemistry, School of Chemical and Life Sciences, Jamia Hamdard, New Delhi-110062, India. E-mail: shamim_chem@yahoo.co.in*

[b]*Department of Pharmacology and Toxicology, National Institute of Pharmaceutical Education and Research, Lucknow-226002, India*

[c]*Centre for Translational &Clinical Research, Jamia Hamdard, New Delhi-110062, India*

[d]*Advanced Instrumentation Research Facility (AIRF), Jawaharlal Nehru University (JNU), New Delhi-110067, India*

to catalyst poisons.[27] Moreover, due to tighter emission legislation in Europe, North America, China and Japan, demand for Pd in the autocatalyst sector has significantly boosted from 114 tonnes in 2009 to 355.9 tonnes in 2019 among which China recorded the highest demand for Pd in 2019.[28,29]

The major source of exposure to Pd is mainly through inhalation by automobile exhaust emissions as over 70% of Pd is applied in the autocatalyst sector.[27,30,31] Although TWCs have been successful in curbing air pollutants to a great level, Pd as a PM is also inevitably emitted into the environment along with other exhaust gases due to abrasion of the alumina (γ-Al_2O_3) washcoat by physical and chemical stress; high temperature and excessive heating.[32–34] Dynamometer experiments carried out on various engines have shown that Pd is emitted from the vehicles at the rate of nanogram per kilometre (100–200 ng km^{-1}).[35] The 99% of released particles on examination were found to be in the metallic state in the inhalable size range of micro-meters (10–0.1 μm).[36,37] Investigations also showed that further disintegration of catalytic convertors fragments also produced fine and ultra-fine particles in the nano-size range (1–100 nm).[38] As a result, very high Pd concentration as high as 1000 ng g^{-1} in the roadside soil has been found near a very busy road, highways and sewage sludges in densely populated areas affecting outdoor workers.[14,39–41] The previous toxicity studies of palladium nanoparticles (PdNPs) have known to show adverse effects in *in vitro* and *in vivo* models.[42] For example, Wilkinson *et al.* evaluated the toxicity effect of palladium nanoparticles (PdNPs) on human primary bronchial epithelial cells (PBEC) and lung carcinoma cells (A549), the results showed dose-dependent cytotoxicity, apoptosis induction and greatly influenced the secretion of inflammation biomarkers such as IL-8 and PGE_2.[26] In another study, Iavicoli *et al.* reported that on the *in vivo* treatment of female Wistar rats to PdNPs sub chronically, the cytokine serum levels were altered, suggesting a harmful effect of PdNPs on the immune system after prolonged exposure.[43]

Dispersion of the contaminated soil due to leaching during rains can further pollute the surface water bodies thus degrading the quality of groundwater and affecting aqueous flora and fauna.[20,44–49] In a study by Speranza *et al.*, on exposing kiwifruit pollen grains to PdNPs, various changes were observed such as a change in their morphology, disrupted plasma membrane, impaired pollen tube and growth by depletion of calcium.[50] Uptake of PdNPs by aquatic life and plants further pose a huge health risk for human consumers as they indirectly become vulnerable to Pd toxicity. Another important route of exposure to Pd is through skin contact in individuals who use dental alloys and jewellery made of Pd metal. Evidence has shown that exposure to PdNPs can enhance the secretion of INF-γ, a T_h1 cytokine involved in type IV immune reactions confirming the increased frequency of allergic sensitization to Pd amongst people living in metropolitan cities.[26,51–53] However, environmental contamination by Pd dental alloys and jewellery is minor.

Nanoparticles having a larger proportion of surface area to volume behaves differently than microparticles when taken up by the organisms *via* inhalation route which is the primary route of exposure. Microparticles having the bigger size when inhaled are generally taken up by lungs and absorbed there whereas nanoparticles having smaller size can diffuse through membranes, have higher uptake in tissues and due to their high mobility, they distribute throughout the body to various organs and even escape the process of endocytosis.[54,55] Therefore, nanoparticles pose a greater threat than microparticles when taken up by the body.

From previous toxicity studies, it has been evident that PdNPs exhibit adverse effects on human health. However, there is still a dire need for more conclusive data by performing risk-assessment studies on various other *in vitro* and *in vivo* models. The extraction of catalyst from catalytic converter fragments to make PdNPs is a difficult and tedious process. Moreover, it is difficult to obtain well defined shape and size distribution. PdNPs have been synthesized by various chemical and physical methods such as sonochemical method, electrochemical method, reverse micelles, wet chemistry and by laser ablation.[56,57] The most common reducing agent to reduce palladium ions (Pd^{2+}) to colloidal Pd^0 in chemical synthesis used is sodium borohydride ($NaBH_4$).[58] However, using $NaBH_4$ is avoided in biological studies since the formed by-product, boric acid, is a bactericide. Green synthesis is gaining much attention these days due to numerous benefits.[59] Green synthesis provides us an eco-friendly platform as compared to chemical methods which involves the use of harsh and toxic chemicals. Chemical methods also have other disadvantages such as high cost, low yields, high temperatures, longer reaction time, short storage time and inflexibility in size control. Whereas synthesis of Pd nanoparticles *via* reduction by plant extract is an eco-friendly and cost-effective method which allows controlled synthesis with well-defined shape and size by altering the pH and reaction temperature, gives higher yields, have shorter reaction time and have three times more stability than nanoparticles prepared by non-green method.[60] Moreover, bio-reduced PdNPs are hydrophilic in nature which can be easily dispersed in aqueous solution and can be further utilised for *in vitro* studies easily. Previously, leaf extracts of soyabean, *cinnamon camfora*, *S. persica* L. (meswak) root, banana peel, *Pelargonium graveolens*, black tea, fenugreek tea and curcuma longa tuber have been successfully utilized in the synthesis of PdNPs and nanoparticles of well-defined shape and size with narrow-distribution have been obtained.[61–66] Therefore, in the present study, we aimed to synthesize PdNPs *via* bio-reduction method using *Parthenium hysterophorus* (PH) leaf extract and further evaluated their toxicity effect on murine macrophages (J774 cell lines). Macrophages are very crucial immune cells found in the reticuloendothelial system which acts as the first line of defence against any foreign particle that invades the body and work by scavenging it through the clearing mechanism called phagocytosis. They are spread throughout the body such as in tissue (histiocyte), liver (Kupffer cells), pulmonary alveoli (Alveolar macrophage), brain and spinal cord (microglia).[67,68] Toxicity parameters such as cell viability, ROS production and induction of apoptosis were investigated. In this study, we also examined the roadside dust of New Delhi for the presence of Pd using

inductively coupled plasma-mass spectroscopy (ICP-MS) technique.

2 Experimental

2.1 Chemicals and reagents

All chemicals purchased were of the highest purity and analytical grade. Palladium(II)chloride ($PdCl_2$, 99%) as the source of palladium ions was received from Loba Chemie Pvt. Ltd. (Mumbai, India) and used without further purification. 1 M HCl solution was prepared to add a known amount of concentrated hydrochloride purchased from Merck (Darmstadt, Germany). *P. hysterophorus* leaves were procured from the Herbal garden located in Jamia Hamdard (New Delhi, India) to make the aqueous leaf extract. All solutions were prepared from Ultrapure water (Milli Q). J774 macrophages cell lines were obtained from American Type Culture Collection (ATCC) through the National Chemical Laboratory (NCL), Pune, India.

2.2 Preparation of *Parthenium hysterophorus* leaf extract

P. hysterophorus (PH) leaves were first thoroughly rinsed in deionised water 2–3 times to get rid of the dirt and impurities and then kept in open and air-dried in shade for 2 days. Then the dried leaves were crushed in a grinder to make a fine powder. 10 g of the powder was weighed and added to 200 mL ultrapure water in a 500 mL beaker and boiled in a water bath for about 15 min. The mixture was cooled down and filtered through Whatman paper no 1 to obtain the aqueous extract. The extract was collected in 50 mL vials and stored in the refrigerator at 4 °C for further use.

2.3 Green synthesis of PdNPs using *P. hysterophorus* leaves

For the synthesis of palladium nanoparticles, 1 mM of $PdCl_2$ solution was prepared by adding 0.0354 g of pure $PdCl_2$ salt in 200 mL of MilliQ water. The solution was stirred for 4 hours and kept overnight for ageing. 10 mL of the aqueous leaf extract was then added to the obtained pale-yellow Pd^{2+} salt solution in a flat-bottom flask and refluxed at 80 °C for 2 hours which were found to be optimum conditions for the synthesis of PdNPs. The colour of the solution gradually changed from pale yellow to brown indicating the formation of PdNPs. The colloidal solution was then centrifuged at 10 000 rpm for 15 min to obtain a black precipitate. Aggregated PdNPs was thus purified by repeated centrifugation for 3 times by Milli-Q water and lastly, freeze-dried in a lyophilizer. The purified PdNPs were then further used for respective *in vitro* toxicity end-point studies.

2.4 Characterisation of PdNPs

The as-prepared *P. hysterophorus* assisted synthesised palladium nanoparticles was first characterized by a double beam Halo DB-20R UV-VIS spectrophotometer using 1 cm quartz cell and wavelength range between 200 to 500 nm. Functional groups of the biomolecules present in the leaf extract were investigated by Cary 630 FTIR instrument (Agilent, USA) in the transmittance mode between 650 and 4000 cm^{-1}. A zetasizer Nano ZS (Malvern, Malvern Instruments Ltd., UK) was used for measuring zeta (ξ) potential of the colloidal solution (conductivity, $\kappa = 1.2$ mS m^{-1} at 25 °C). Under surface morphology studies, high-resolution transmission electron microscopy (HRTEM) and selective area electron diffraction (SAED) of Pd-NPs was carried out on JEOL 2100F at 100 keV. Further, field emission scanning electron micrograph and elemental composition of PdNPs surface (FESEM) was obtained through FEI Quanta 200 F SEM equipped with Oxford-EDX system IE 250 × Max 80. Finally, crystallographic studies were done on X-ray diffractometer (PANalytical X'Pert Pro) in the angle range of 20–80° with a scan rate of 1° min^{-1} operated at 30 mA current and voltage of 40 kV with CuKα (1.5418 Å) radiation.

2.5 Dust sample collection and analysis

Road dust samples were collected from different parts of New Delhi during fall in November 2019 under the sunny sky. Locations of Dhaula Kuan, I.T.O, Anand Vihar, Azad market was chosen based on their heavy traffic pattern. Busiest main roads, adjacent lanes, road dividers and intersections were aimed to monitor the lateral distribution of Pd. 500 g of dust samples were collected carefully from each area in polythene bags using gloves and the bags were sealed. The dust samples were then sent to the lab of AGSS analytical Pvt. Ltd. (New Delhi) for its analysis by ICP-MS technique.

2.6 Cell culture

The *in vitro* study was carried out using the murine macrophage cell line, J774 (American Type Culture Collection, Rockville, MD). Confluent macrophages were subcultured and maintained at 37 °C in Dulbecco's modified Eagle's medium (Sigma, St. Louis, MO) under a humidified atmosphere (5% CO_2). All media were supplemented with 10% fetal calf serum (Hyclone, Logan, UT), and antibiotic (Sigma) containing 50 U mL^{-1} of penicillin and 50 mg mL^{-1} of streptomycin and actinomycin.

2.7 MTT assay

Cytotoxicity of Pd-NPs was evaluated using MTT assay as previously described by Naqvi *et al.*[69] J774 cells were seeded in flat-bottomed 96-well plates at a density of 1×10^5 mL^{-1} cells. Different concentrations (25, 100, 200, 300, 400, and 500 μg mL^{-1}) of palladium nanoparticles were prepared and then added to the plate and incubated for 24 hours in the medium. The media was removed after incubation and 90 μL of the fresh media was added per well to the cells after washing it thoroughly with sterile phosphate-buffered saline to remove unreacted PdNPs. 10 μL (5 mg mL^{-1} stock) of MTT reagent (3-(4,5-dimethylthiazol-2-yl)-2,5-diphenyltetrazolium bromide; Roche Diagnostic, Mumbai, India) was then added per well and the plate was incubated for six hours in an incubator. After incubation, the media was discarded from the wells again and 100 μL of dimethyl sulfoxide (DMSO) was added to solubilize the purple coloured formazan crystals. With the help of Bio-Rad enzyme-linked immunosorbent assay reader, the level of the purple coloured formazan derivative was determined on a reader at a wavelength of 490 nm (reference wavelength 650

nm). Data are expressed as percentage viability of the cells and it was calculated as the ratio of mean absorbance of triplicate readings with respect to mean absorbance of control wells.

2.8 Lactate dehydrogenase leakage (LDH) assay

LDH assay is another determinant for the potential cytotoxicity exerted by PdNPs. For this, LDH release into the extracellular space was monitored by the CytoTox 96 nonradioactive cytotoxicity assay (Promega, Madison, WI). The method involves placing cells (2×10^4 cells per mL) in 24-well plates and incubating it with different concentration of Pd-NPs (25–500 μg mL^{-1}) for three and six hours. The plates were then centrifuged, and aliquots (50 μL) of cell culture medium were collected from each well and placed in new microtiter plates. Finally, 50 μL of substrate solution was added to each well and the plates incubated for 30 minutes at room temperature. The absorbance at 490 nm as measured with a microplate reader. Each experiment was done in triplicate. Cytotoxicity is expressed relative to the basal lactate dehydrogenase release by untreated control cells.

2.9 Apoptotic assay

The apoptotic assay was done to measure the longevity of a cell in culture as previously described by Naqvi *et al.*[69] For this method, the apoptotic cells were first stained with fluorescent dye Hoechst-33342 (Roche), an apoptotic marker and then counterstained by propidium iodide. The cells were plated and grown in six-well and twelve-well plates (TPP, Trasadingen, Switzerland) at a density of 2×10^4 cells per well containing serum-free medium until they were subconfluent at 37 °C at 95% CO_2. Further, the cells were incubated with 25, 200 and 500 μg mL^{-1} Pd-NPs for three and six hours respectively. However, for the control group, nanoparticles were not added to the cells and incubated for the same time periods. It was made sure to collect 500 μL of the culture supernatant before terminating the culture from each well for further biochemical assays. To properly stain the cells, they were incubated for 15 minutes with Hoechst-33342 (Roche) at a working dilution of 5 mM and propidium iodide at a final concentration of 50 μg mL^{-1}. Hoechst-33342 is a dye that is used to stain the nuclei in a blue shade and is also extensively used as an apoptotic marker in the apoptotic assay.[70] After staining, cells were washed in phosphate-buffered saline three times for five minutes each, and the coverslips were mounted on slides with 10% glycerol in phosphate-buffered saline. The cells were immediately observed under an upright fluorescent microscope (Eclipse 600; Nikon, Melville, NY) with 488 nm and 350 nm filters, and images were captured using an Olympus DP-71 digital camera (Olympus, Centre Valley, PA) mounted on the microscope. Ten different fields were captured at 40×, and subsequently cell counts were taken within the fields to get statistically significant counts for apoptotic cells and viable cells, in each case. The apoptotic cells were quantified as a percentage of the total cell count. Data analysis was performed using Excel (Microsoft Corp., Redmond, WA).

2.10 H_2DCFDA assay

This assay was performed to detect the reactive oxygen species intermediates in murine macrophages as previously reported by Naqvi *et al.*[69] J774 cells were grown on coverslips at a density of 2×10^4 cells per well until subconfluent. A peroxide-sensitive fluorescent probe, carboxy-2′,7′-dichlorofluorescein diacetate (H_2DCFDA; Invitrogen, Carlsbad, CA) was used to measure intracellular ROS. The cells were loaded with 20 μM H_2DCFDA for 60 minutes at 37 °C. After 60 minutes, the cells were thoroughly washed and fresh media was added. The cells were incubated with Pd-NPs at 400 μg mL^{-1} and 500 μg mL^{-1} under standard conditions. After the defined time points, the cells were washed with sterile phosphate-buffered saline and mounted on glycerol phosphate-buffered saline. The cells were observed under a fluorescent microscope (Eclipse 600; Nikon) with a green filter, and the images were captured with a DP-71 digital camera (Olympus). Cells incubated without Pd-NPs were used as a negative control, and 100 μM H_2O_2 was used as a positive control.

2.11 Statistical analysis

Statistical analyses were performed using the Student's *t*-test for unpaired data, and *P* values <0.05 were considered statistically significant. Data are presented as means ± standard error of the mean.

3 Results and discussion

In the present study, we investigated the potential hazardous effects of bio-synthesized PdNPs prepared *via* bio-reduction by aqueous leaf extract of *P. hysterophorus* plant species on murine macrophage cell line (J774). *Parthenium hysterophorus* (PH), also

Fig. 1 *Parthenium hysterophorus* (Asteraceae family).

known as carrot gas, is a noxious species of weed commonly found in India as well as other parts of Asia and is known to be highly invasive in nature and toxic to the vegetation crops, livestock and humans (Fig. 1).[71] Chemical analysis and photochemical screening of *P. hysterophorus* leaf has shown that it consists of primary and secondary metabolites such as sesquiterpene lactones like parthenin, alkaloid, steroid, flavonoid like quercetagetin, phenols like caffeic acid, vanillic acid, *p*-coumaric acid, glycosides, protein and carbohydrates.[71,72] According to FT-IR spectroscopy data studies, it has been reported that naturally occurring phenols in terpenoids and pi-electrons in flavonoids are involved in the chelation and reduction of metal ions. It has been suggested that pi-electrons of carboxyl group (C=O) in flavonoids reduces metal ions by donating electrons to the free 5s orbital of the metal ion. Moreover, hydroxyl group present in phenols itself gets oxidized by donating proton and reduces the metal ion into a free metal.[60,73] An attempt was made to utilise this ubiquitous weed for a better purpose by exploiting the reducing and capping properties of their primary and secondary metabolites.

The reduction of aqueous Pd(II) to Pd^0 was first visually observed by the gradual change in colour of the Pd^{2+} salt solution from pale yellow to dark brown upon addition of aqueous leaf extract as shown in Fig. 2 (inset image). The colour change is due to the surface plasmon resonance (SPR), a property unique to metallic nanoparticles having free electrons oscillating on its surface.[74] To further confirm the formation of PdNPs and to determine its shape, size, particle size distribution, crystallinity and stability the following characterization methods were done.

3.1 UV-Vis spectra of Pd-NPs

The formation of bio-fabricated PdNPs was initially confirmed by UV-Visible spectroscopy scanned in the wavelength range of 200–500 nm. For this, UV-Vis spectra of pure $PdCl_2$ and PdNPs was recorded (Fig. 2). $PdCl_2$ shows a characteristic absorption band around 415–420 nm which could be due to d–d transition of Pd(II) ions (d8 configuration) and the disappearance of the band and appearance of a broad and continuous spectrum above 400 nm signifies the formation of PdNPs (Pd^0). This data is in agreement with the previous studies done by using different biological material for the reduction process.[61–64,75]

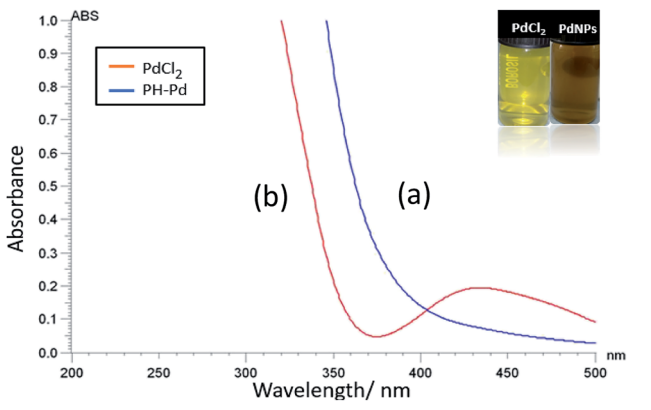

Fig. 2 UV-Visible absorption spectra of (a) PdNPs (PH–Pd) prepared by bio reduction of Pd^{2+} with *P. hysterophorus* leaves extract (blue line) (b) palladium chloride salt solution (Pd^{2+}) showing its characteristic absorption peak around 420 nm (red line). The inset shows a digital image of pale-yellow palladium chloride solution before reduction and dark brown as-prepared colloidal solution of Pd.

3.2 FT-IR analysis (formation mechanism of PdNPs)

Earlier studies on the biogenic synthesis of metal NPs have shown that primary and secondary metabolites present in plant extracts perform the dual function as a reducing agent as well as a capping agent in the biosynthesis of metal nanoparticles from their ions.[61–64,73] For this purpose, FT-IR analysis of the plant extract (P.E) and dried PdNPs was carried out to confirm these studies and to identify which biomolecules present in PH are acting as reducing and capping agent (Fig. 3). The hydroxyl functional group present in phenolic acids, terpenoids and flavonoids was confirmed by the broad peak observed in the range of 3100–3500 cm^{-1} in both spectrums. Studies have shown that hydroxyl group plays an important role in the redox reaction by giving up its proton and reducing the metal ion and flavonoids exhibit good chelating property by which it caps the nanoparticle through C and O elements.[73] A peak at ~2940 cm^{-1} suggests the presence of –CH group in PdNPs IR spectrum. On comparing both spectrums, there was a shift in peak from ~1643 to ~1631 cm^{-1} suggests C=C stretching frequency and some additional peaks at ~1246 cm^{-1} and ~1045 cm^{-1} (C–O stretching frequency). Plant extract (P.E.) spectra and pure PdNPs spectra were found to have similar absorption bands either at the same position or with a slight shift. These findings clearly suggest that residual organic moieties of the PH aqueous leaf extract functioned as a capping ligand on the surface of PdNPs and was also actively involved in the reduction process of the metal ion.

3.3 Crystalline phase analysis

Powder XRD diffraction analysis was carried out to confirm the crystallinity of biosynthesized PdNPs. The pattern showed three major Bragg reflections at 40.31°, 46.8°, and 68.2° which corresponds to (111), (200), (220) (Fig. 4). These peaks

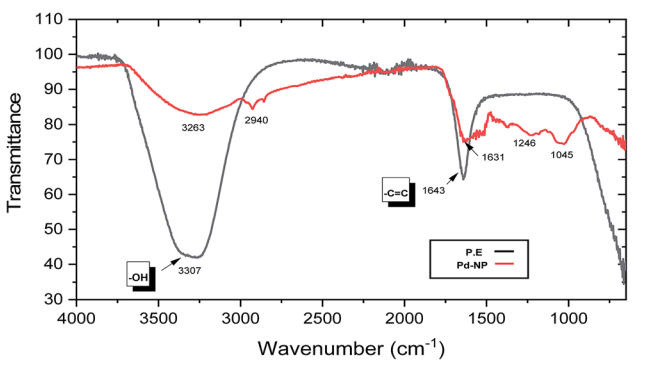

Fig. 3 Fourier-transform infrared spectra (FT-IR) of (a) aqueous PH Plant extract (P.E, black line) (b) PH reduced PdNPs.

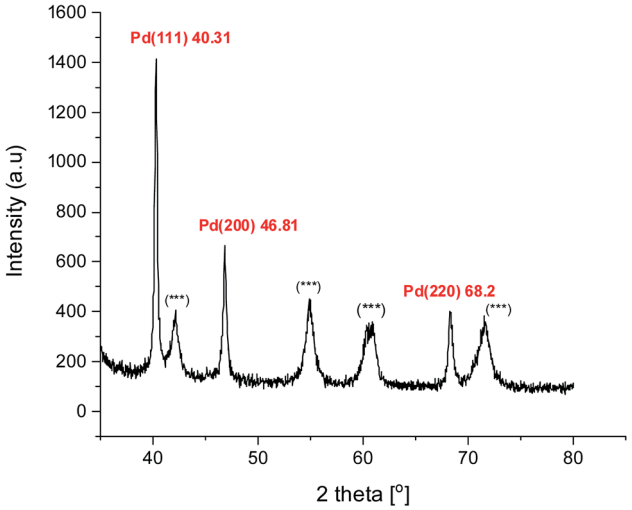

Fig. 4 XRD diffraction pattern of as-synthesized green PdNPs.

correspond to the face-centred cubic (fcc) lattice crystalline structure of metallic Pd^0. A similar pattern of green synthesized PdNPs has been observed in the previous studies.[61,63,75] The most significant peak was found to be of (111) plane at $2\theta = 40.31°$ by which, we infer that this could be the dominant orientation of green PdNPs. As the peak width is inversely proportional to the crystallite size, the observed broadened peaks could be due to the small size of nanoparticles formed. Along with crystallinity, powder XRD also gave us an idea about the average particle size (~4 nm) of the Pd crystallites based on the full width half maximum (FWHM) of the most intense peak ($2\theta = 40.31°$) using Debye–Scherrer's equation.[76] Also, some additional peaks (***) were observed in the diffraction pattern, apart from the reflections from crystalline PdNPs, this could be possibly due to the presence of crystalline biomolecules present in the PH leaf extract.[63,75] These extra peaks further prove that the organic moieties of the parthenium P.E. play an important role as a capping agent around crystalline PdNPs.

3.4 Surface morphology, size analysis and particle distribution

High-resolution transmission electron microscopy (HR-TEM) and scanning electron microscopy (SEM) was recorded to investigate the morphology and size of green synthesized PdNPs. The overview of HRTEM images and the size distribution of particles is given in Fig. 5(A)–(D). It was found that *P. hysterophorus* assisted PdNPs were mostly spherical, monodispersed and have an average size of 3.6 nm ± 1.13 (Fig. 5(D)). It was interesting to notice fringe lattice pattern when the TEM image was magnified to 1 nm scale (Fig. 5(B)) which further goes to show the crystallinity of PdNPs. SEM images show an irregular shaped cluster of nanoparticles formed by aggregation of smaller spherical particles (Fig. 6). By the images, taking a look closely at the light contrast it can also be inferred that an organic layer is present and PdNPs might be chelated by bio-organic moieties capping the nanoparticle and acting as a stabilizing agent.

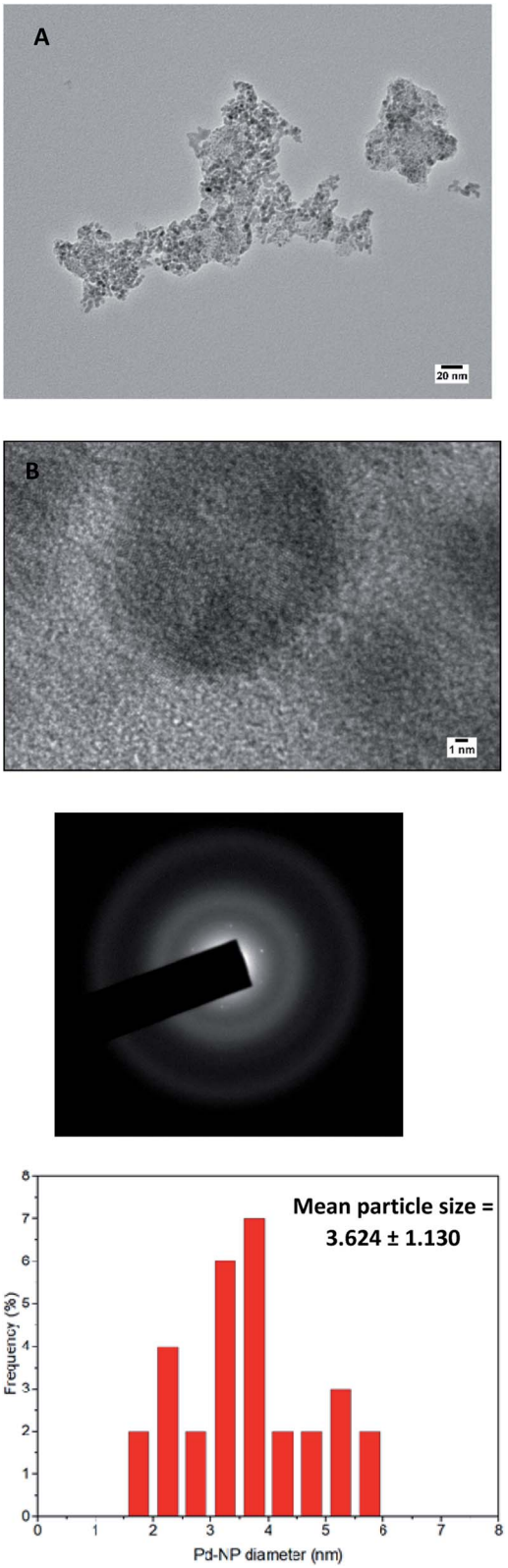

Fig. 5 (a) and (b) High resolution transmission electron microscopy (HR-TEM) of bio-synthesized PdNPs. (c) Selective area electron diffraction (SAED) pattern (d) particle size distribution graph.

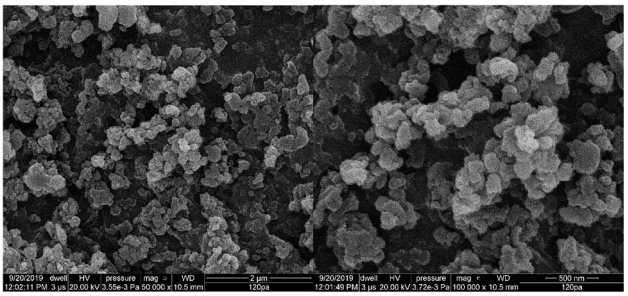

Fig. 6 Scanning electron microscopy (SEM) images of green fabricated PdNPs.

3.5 SAED, elemental composition and stability studies of PdNPs

The face centred cubic lattice of green synthesized PdNPs was further confirmed by selected area electron diffraction (SAED) pattern. Three concentric well-defined rings were observed in the pattern which confirms the (111), (200) and (220) Bragg's reflection planes in XRD whereas the bright spots forming an inner ring signifies that PdNPs are crystalline (Fig. 5(C)).

The elemental composition of biosynthesized PdNPs was determined by energy-dispersive X-ray spectroscopy (EDS/EDX).

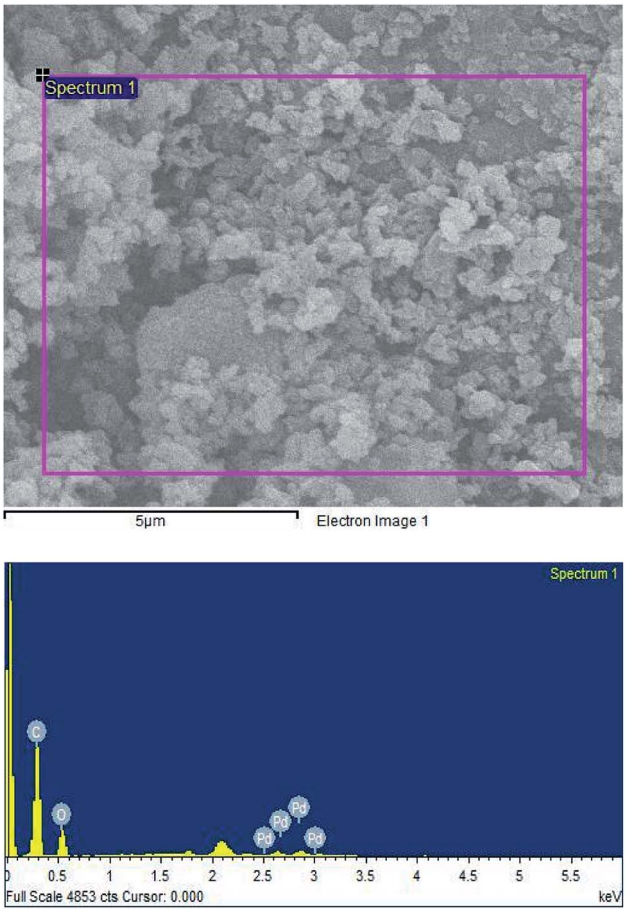

Fig. 7 The EDS spectrum of *P. hysterophorus* reduced PdNPs.

PdNPs formation was confirmed by the presence of Pd peaks between the region of 2.5–3 keV. Along with Pd, strong C and O peaks were also observed further solidify the dual action of plant metabolites of PH acting as a capping agent and a reducing agent (Fig. 7).

To determine the stability and surface charge of the formed aqueous nano-suspension of Pd, zeta potential measurements of PdNPs were carried out at 25 °C through dynamic light scattering (DLS) technique. Zeta potential values of nanoparticles between >25 mV or <−25 mV are considered to have stable structures.[67] Zeta potential analysis of PdNPs showed the average negative surface charge of −11.3 mV which signifies that formed green synthesized PdNPs are stable in aqueous solution (Fig. 8).

3.6 Measurement of Pd concentration in dust samples by ICP-MS technique

The data of dust samples from four different heavy travelled regions (Dhaula Kuan, I.T.O, Anand Vihar, Azad market) from New Delhi were collected and analysed by ICP-MS technique. Presence of Palladium concentration was confirmed in the roadside soil and was found to be in the range of 571.483–805.37 ng g^{-1}. Roadside soil of Dhaula Kuan was found to have maximum Pd concentration *i.e.* 805.37 ng g^{-1}. These values were found to be way above than the upper crust values of PGE and quite higher as compared to the other studies done in other polluted cities of the world.

3.7 Bio-synthesized palladium nanoparticles show cytotoxic effects against murine macrophages

To analyse and evaluate the potential toxic effects of PdNPs, murine macrophage J774 cell line was procured and used as a model to simulate macrophages which forms an essential part of the mononuclear phagocytic system (MPS). Macrophages are spread throughout the body and play a crucial role in regulating homeostasis. In the event of foreign particle invasion (in this case, PdNPs), it gets activated by the immune system and acts as a primary defence system by destroying the particle and initiating the immune response.[67] Thus, it is important to understand the effect of PdNPs on our immune system and how does it respond when particulate matter is inhaled or ingested.

In the first endpoint study, cell viability and cell proliferation of dose-dependent PdNPs was determined by MTT assay. MTT assay works by conversion of yellow water-soluble tetrazolium dye into insoluble purple formazan crystals by mitochondrial succinate dehydrogenase enzymes which indirectly tells us about the cell metabolic activity.[77] For this purpose, exponentially growing cultures of J774 cells were exposed to increasing concentrations of PdNPs (25, 100, 200, 300, 400 and 500 µg mL^{-1}) and cell viability was assessed after 24 hours. Results of MTT assay showed a dose-dependent decrease in the viability of cells (Fig. 9). At 25 µg mL^{-1} concentration, the viability of cells at six hours was 90%, between 100–300 µg mL^{-1} insignificant reduction was observed with only 2–5% reduction. However, on increasing concentration to 400 and 500 µg mL^{-1} significant decrease in cell viability was noted where 60% cell viability was

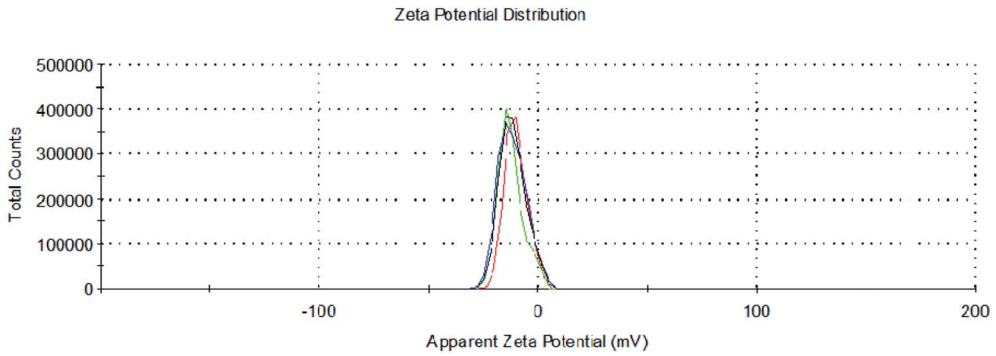

Fig. 8 Zeta potential measurement graph of PdNPs.

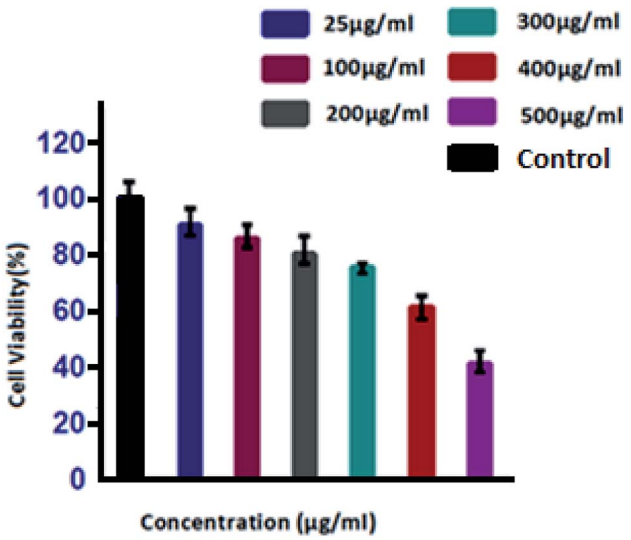

Fig. 9 The effects of palladium nanoparticles on cell proliferation and viability of J774 cells as determined by MTT assay. Concentration dependent cytotoxic effects of nanoparticles evaluated after 24 hours of incubation. Results are represented as means ± standard error of the mean. Note: *significant difference from control ($P < 0.05$).

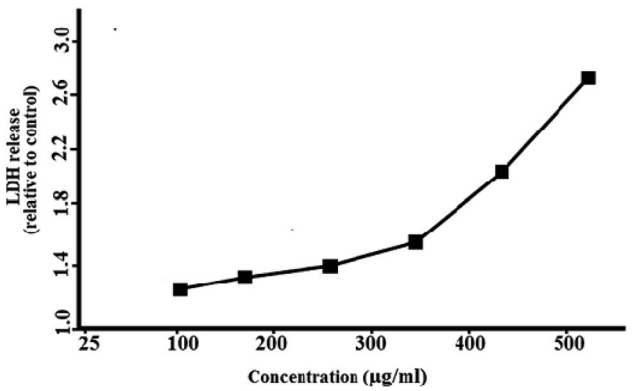

Fig. 10 Concentration dependent membrane damage as determined by lactate dehydrogenase leakage from J774 cell lines (2×10^4 cells per mL) incubated with PdNPs for six hours.

seen for former concentration and 40% for the latter. This shows PH coated PdNPs (~4 nm) exhibit cytotoxic effects on J774 cells at higher doses (400 and 500 µg mL^{-1}).

3.8 Bio-synthesized palladium nanoparticles disrupt the cell membrane integrity of J774 cells

Lactate dehydrogenase (LDH) also called a cell death marker is a stable and soluble enzyme found in the cytoplasm of normal cells. When the cell loses its membrane integrity on necrosis it releases LDH enzyme into extracellular space which indicates damaged cell or cell death. For this, LDH assay was carried out by exposing green synthesized PdNPs having different concentrations (25–500 µg mL^{-1}) to J774 cells for six hours respectively. Results showed significant release in LDH levels at higher concentrations (400 and 500 µg mL^{-1}) of PdNPs when incubated for six hours (Fig. 10). MTT assay supported these findings. This indicated that bio-synthesized PdNPs when exposed to J774 cells leads to cell membrane injury at higher doses and is time and dose-dependent (Table 1).

Table 1 Measured Pd concentration from different parts of New Delhi

Area	Type	Location	C_{Pd} (µg kg^{-1})
Dhaula Kuan	Dust	Roadside	805.379
I.T.O	Dust	Roadside	571.483
Anand Vihar	Dust	Roadside	591.243
Azad market	Dust	Roadside	782.301

Table 2 Apoptosis indices of J774 cells following incubation with 25, 200, and 500 µg mL^{-1} of bio-synthesized PdNPs for three and six hours

Nanoparticle concentration (µg mL^{-1})	Three hours	Six hours
Control	1.4 ± 0.3	1.6 ± 0.3
25	1.8 ± 0.6	2.3 ± 0.8
200	2.4 ± 1.2	27.6 ± 2.5[a]
500	24.8 ± 3.5	38.4 ± 6.3[a]

[a] Note: $P < 0.001$.

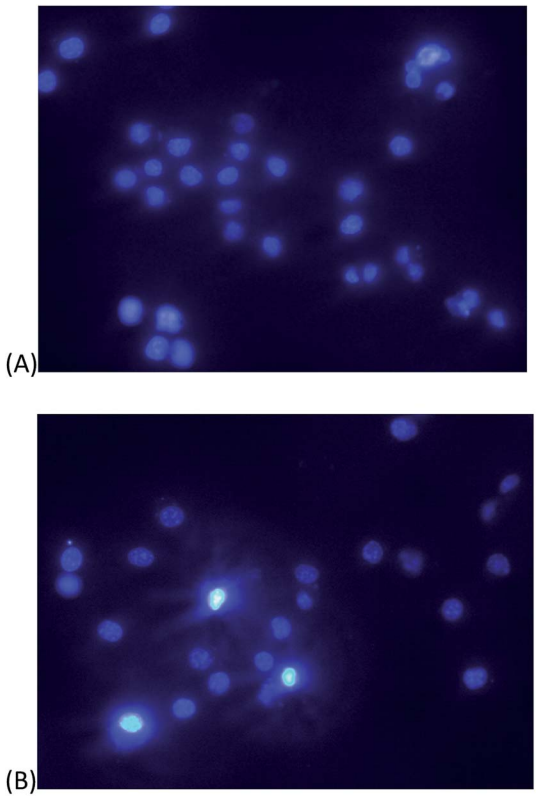

Fig. 11 Apoptosis of J774 cells incubated with 500 μg mL^{-1} palladium nanoparticles (A) control (B) at six hours. The bright blue nuclei represent apoptosis stained with fluorescent dye Hoechst-33342.

3.9 Biosynthesized PdNPs induce apoptosis in J774 cells

Apoptosis is a series of well-organised events of cell programmed death which occurs by activation of a protease called as caspases and involves shrinking of cytoplasm, membrane blebbing, chromosome condensation, cleavage of DNA and finally engulfed by phagosomes.[78] The apoptotic assay is a technique that detects these events and measures the extent of apoptosis by apoptotic index. Staining of the cell with apoptotic markers like Hoechst dye and propidium iodide (PI) is carried out. Hoechst-33342 signifies early apoptosis without even permeating the cell membrane by labelling the nuclei bright blue which is a clear indication of apoptotic cells whereas uniform blue nuclei do not show apoptosis.[69,70] PI only enters dead cells with the damaged cell membrane. Three doses (25, 200, 500 μg mL^{-1}) of PdNPs incubated for three and six hours were taken and their behaviour was observed on the integrity of DNA of macrophages. At 500 μg mL^{-1}, moderate apoptosis was observed indicated by the fluorescent blue nuclei, however, at lower doses apoptosis was not that significant. Table 2 shows apoptosis indices of J774 cells at three and six hours with 25, 200 and 500 μg mL^{-1} of green synthesized PdNPs. For control, the indices at three and six hours were 1.4 ± 0.3 and 1.6 ± 0.3. At 25 μg mL^{-1}, the indices at three and six hours increased to 1.8 ± 0.6 and 2.3 ± 0.8. For 200 μg mL^{-1} concentration, after 3 hours the index was 2.4 ± 1.2 but after 6 hours the index drastically increased to 27.6 ± 2.5, however, the apoptotic index was seen highest for concentration at 500 μg mL^{-1} after six hours which shows apoptosis is time and dose-dependent. Fig. 11 shows the apoptosis images of J774 cells incubated with 500 μg mL^{-1} PdNPs at control conditions and for six hours. The bright blue nuclei represent apoptosis stained with fluorescent dye Hoechst-33342. Interestingly, only moderate level of apoptosis was observed.

3.10 Biosynthesized PdNPs induce ROS generation in J774 cells

High oxidative stress caused by increased levels of reactive species (ROS) inside the cell could induce DNA damage and apoptosis. To detect the levels of generated ROS levels in J774 cells by the green synthesized PdNPs, 2′,7′-dichlorodihydrofluorescein diacetate (H_2DCFDA) test was performed. When the non-fluorescent H_2DCFDA is oxidized by ROS, it converts to the highly fluorescent 2′,7′-dichlorofluorescein (DCF). The intensity of highly fluorescent DCF trapped intracellularly act as a marker for generated oxidative stress. When PdNPs of concentration 500 μg mL^{-1} were incubated in J774 cells for six hours, the images showed distorted and smudged cell morphology of high green fluorescent intensity (Fig. 12). However, only moderate levels of ROS generation were inflicted by PdNPs. This may be explained by the anti-oxidant effect exhibited by PdNPs as demonstrated in the previous studies.[79,80] Similar observations were noted on previous toxicity studies on A549 cells by Wilkinson *et al.*[26]

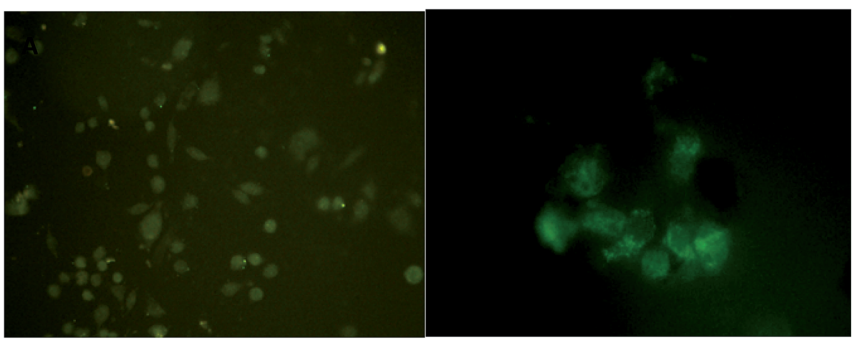

Fig. 12 H2DCFDA assay for intracellular reactive oxygen species with palladium nanoparticles (A) control and (B) at concentration of 500 μg mL^{-1} at six hours.

4. Conclusions

This study presents a risk assessment model of bio-engineered PdNPs on murine macrophages. In this study, an aqueous leaf extract of *Parthenium hysterophorus* plant was utilized for the bio-reduction and stabilization of PdNPs. By this cheap and eco-friendly method, a well-defined spherical and crystalline PdNPs of size ~4 nm were obtained with a narrow size distribution. Characterization studies of PH capped PdNPs such as TEM, FT-IR, XRD and EDX clearly suggested the significant role of plant metabolites such as phenols, terpenoids and flavonoids in the reduction and stabilization of PdNPs.

Dose-dependent and time dependent toxicity evaluation of pure PdNPs was investigated on J774 cell lines (murine macrophages) and *in vitro* end points such as cytotoxicity assays (MTT and LDH), apoptosis and free radical generation (H_2DCFDA) were accomplished. Results suggested that PdNPs showed low cell viability, induced apoptosis and ROS generation at concentrations of 400 and 500 μg mL^{-1} when incubated for six hours. This preliminary data of our *in vitro* studies gives us the overview and significant information on the interaction of PdNPs with macrophages. With more automobiles on the road and to meet the stricter emission regulations in various countries in order to control the automobile exhaust pollutants, mining of PGMs is going to further increase leading to more imbalance in the biogeochemical cycles of metals in the environment. Such high and continuous exposure of PdNPs to the general population mainly outdoor workers and flora and fauna can lead to morbidity to chronic respiratory diseases and pulmonary diseases in a long term. Hence, risk assessment studies of Pd and other PGMs are highly necessary to regulate their usage in the catalytic converters in order to ensure safe and sustainable technology.

Funding

This research did not receive any specific grant from funding agencies in the public, commercial, or not-for-profit sectors.

Conflicts of interest

All authors declare that they have no conflict of interests related to this study.

Abbreviations

ROS	Reactive oxygen species,
XRD	X-ray powder diffraction
HR-TEM	High-resolution transmission electron microscopy
ICP-MS	Inductively coupled plasma mass spectroscopy
SEM	Scanning electron microscopy
H2DCFDA	2′,7′-Dichlorodihydrofluorescein diacetate
EDX	Energy-dispersive X-ray spectroscopy
FT-IR	Fourier transform infrared spectroscopy

Acknowledgements

Advanced Instrumentation Research Facility (AIRF), Jawaharlal Nehru University (JNU), New Delhi, India, Central Research Facility, IIT Delhi, AGSS analytical Pvt. Ltd., Central Instrumentation Facility of Jamia Hamdard and Jamia Milia Islamia, New Delhi are gratefully acknowledged for their contribution.

References

1 World Health Organization, https://www.who.int/mediacentre/news/releases/2014/air-pollution/en/, (accessed November 2020).
2 The New York Times, https://www.nytimes.com/2016/06/27/business/energy-environment/study-links-6-5-million-deaths-each-year-to-air-pollution.html, (accessed November 2020).
3 F. Karagulian, C. A. Belis, C. F. C. Dora, A. M. Prüss-Ustün, S. Bonjour, H. Adair-Rohani and M. Amann, *Atmos. Environ.*, 2015, **120**, 475–483.
4 The Times of India, https://timesofindia.indiatimes.com/city/delhi/usual-suspects-vehicles-industrial-emissions-behind-foul-play-all-year/articleshow/66228517.cms, (accessed on November 2020).
5 J. Huang, Q. Liu and X. Guo, in *Encyclopedia of Environmental Health*, Elsevier, 2019, pp. 655–662.
6 K. Hans Wedepohl, *Geochim. Cosmochim. Acta*, 1995, **59**, 1217–1232.
7 C. R. M. Rao and G. S. Reddi, *Trac. Trends Anal. Chem.*, 2000, **19**, 565–586.
8 A. B. Patil and B. M. Bhanage, *J. Nanosci. Nanotechnol.*, 2013, **13**, 5061–5068.
9 K. H. Ek, G. M. Morrison and S. Rauch, *Sci. Total Environ.*, 2004, **334–335**, 21–38.
10 I. S. Sen and B. Peucker-Ehrenbrink, *Environ. Sci. Technol.*, 2012, **46**, 8601–8609.
11 O. Morton, H. Puchelt, E. Hernández and E. Lounejeva, *J. Geochem. Explor.*, 2001, **72**, 223–227.
12 F. Zereini, C. Wiseman and W. Püttmann, *Environ. Sci. Technol.*, 2007, **41**, 451–456.
13 J. Wang, R. Zhu and Y. Shi, *J. Environ. Sci.*, 2007, **19**, 29–34.
14 R. Mathur, V. Balaram, M. Satyanarayanan, S. S. Sawant and S. L. Ramesh, *J. Environ. Earth Sci.*, 2011, **62**, 1085–1098.
15 R. Djingova, P. Kovacheva, G. Wagner and B. Markert, *Sci. Total Environ.*, 2003, **308**, 235–246.
16 Y. A. Pshenichkina and A. Y. Pshenichkin, *Contemp. Probl. Ecol.*, 2018, **11**, 221–226.
17 D. S. Lee, *Nature*, 1983, **305**, 47–48.
18 I. Thornton, *et al.*, Pollutants in urban waste water and sewage sludge, *Office for official publications of European communities*, 2001, cited 2020, October 9.
19 K. Kanitsar, G. Koellensperger, S. Hann, A. Limbeck, H. Puxbaum and G. Stingeder, *J. Anal. At. Spectrom.*, 2003, **18**, 239–246.
20 S. Zimmermann, A. von Bohlen, J. Messerschmidt and B. Sures, *J. Helminthol.*, 2005, **79**, 85–89.

21 K. H. Ek, S. Rauch, G. M. Morrison and P. Lindberg, *Sci. Total Environ.*, 2004, **334–335**, 149–159.
22 C. Barbante, A. Veysseyre, C. Ferrari, K. Van De Velde, C. Morel, G. Capodaglio, P. Cescon, G. Scarponi and C. Boutron, *Environ. Sci. Technol.*, 2001, **35**, 835–839.
23 T.-O. Soyol-Erdene, Y. Huh, S. Hong and S. D. Hur, *Environ. Sci. Technol.*, 2011, **45**, 5929–5935.
24 G. J. K. Acres and B. Harrison, *Top. Catal.*, 2004, **28**, 3–11.
25 G. Winterstein, G. Stahn, M. Voigt, M. Kühn and G. Ceramic, *Ceram. Forum Int.*, 1998, **75**, 8–16.
26 K. E. Wilkinson, L. Palmberg, E. Witasp, M. Kupczyk, N. Feliu, P. Gerde, G. A. Seisenbaeva, B. Fadeel, S.-E. Dahlén and V. G. Kessler, *ACS Nano*, 2011, **5**, 5312–5324.
27 K. Ravindra, L. Bencs and R. Van Grieken, *Sci. Total Environ.*, 2004, **318**, 1–43.
28 J. Matthey, *Platinum Met. Rev.*, 2010, **54**(3), 192–193.
29 J. Matthey, *PGM market report*, May 2020, pp. 35–37, available from: https://matthey.com/en/news/2020/pgm-market-report-may-2020.
30 S. Rauch, H. F. Hemond, C. Barbante, M. Owari, G. M. Morrison, B. Peucker-Ehrenbrink and U. Wass, *Environ. Sci. Technol.*, 2005, **39**, 8156–8162.
31 G. J. K. Acres and B. Harrison, *Top. Catal.*, 2004, **28**, 3–11.
32 M. Moldovan, M. Milagros Gómez and M. Antonia Palacios, *J. Anal. At. Spectrom.*, 1999, **14**, 1163–1169.
33 M. A. Palacios, M. M. Gómez, M. Moldovan, G. Morrison, S. Rauch, C. McLeod, R. Ma, J. Laserna, P. Lucena, S. Caroli, A. Alimonti, F. Petrucci, B. Bocca, P. Schramel, S. Lustig, M. Zischka, U. Wass, B. Stenbom, M. Luna, J. C. Saenz, J. Santamaría and J. M. Torrens, *Sci. Total Environ.*, 2000, **257**, 1–15.
34 F. Zereini, H. Alsenz, C. L. S. Wiseman, W. Püttmann, E. Reimer, R. Schleyer, E. Bieber and M. Wallasch, *Sci. Total Environ.*, 2012, **416**, 261–268.
35 S. Artelt, H. Kock, H. P. König, K. Levsen and G. Rosner, *Atmos. Environ.*, 1999, **33**, 3559–3567.
36 R. Schlogl, G. Indlekofer and P. Oelhafen, *Angew. Chem., Int. Ed.*, 1987, **26**, 309–319.
37 S. Artelt, K. Levsen, H. P. Konig and G. Rosner, *Engine test bench experiments to determine platinum emissions from three-way catalytic converters*, Springer-Verlag, Berlin, 2000, pp. 33–44.
38 H. M. Prichard and P. C. Fisher, *Environ. Sci. Technol.*, 2012, **46**, 3149–3154.
39 M. Jackson, J. Sampson and H. Prichard, *Sci. Total Environ.*, 2007, **385**, 117–131.
40 J. D. Whiteley and F. Murray, *Sci. Total Environ.*, 2003, **317**, 121–135.
41 K. Leopold, M. Maier, S. Weber and M. Schuster, *Environ. Pollut.*, 2008, **156**, 341–347.
42 V. Leso and I. Iavicoli, *Int. J. Mol. Sci.*, 2018, **19**, 503.
43 I. Iavicoli, L. Fontana, V. Leso, M. Corbi, A. Marinaccio, K. Leopold, R. Schindl, D. Lucchetti, F. Calapà and A. Sgambato, *Hum. Exp. Toxicol.*, 2018, **37**, 309–320.
44 J. Schäfer, D. Hannker, J.-D. Eckhardt and D. Stüben, *Sci. Total Environ.*, 1998, **215**, 59–67.
45 B. Sures, S. Zimmermann, J. Messerschmidt and A. von Bohlen, *Ecotoxicology*, 2002, **11**, 385–392.
46 S. Zimmermann, J. Messerschmidt, A. von Bohlen and B. Sures, *Environ. Res.*, 2005, **98**, 203–209.
47 P. Göbel, C. Dierkes and W. G. Coldewey, *J. Contam. Hydrol.*, 2007, **91**, 26–42.
48 S. Lüderwald, F. Seitz, G. A. Seisenbaeva, V. G. Kessler, R. Schulz and M. Bundschuh, *Bull. Environ. Contam. Toxicol.*, 2016, **97**, 153–158.
49 I. Bednarova, H. Mikulaskova, B. Havelkova, L. Strakova, M. Beklova, J. Sochor, D. Hynek, V. Adam and R. Kizek, *Neuroendocrinol. Lett.*, 2014, **2**(suppl. 35), 35–42.
50 A. Speranza, K. Leopold, M. Maier, A. R. Taddei and V. Scoccianti, *Environ. Pollut.*, 2010, **158**, 873–882.
51 A. Cristaudo, V. Bordignon, F. Petrucci, S. Caimi, M. De Rocco, M. Picardo, P. C. Fei and F. Ensoli, *Int. J. Immunopathol. Pharmacol.*, 2009, **22**, 605–614.
52 J. T. Minang, I. Areström, M. Troye-Blomberg, L. Lundeberg and N. Ahlborg, *Clin. Exp. Immunol.*, 2006, **146**, 417–426.
53 B. Santucci, C. Valenzano, M. de Rocco and A. Cristaudo, *Contact Dermatitis*, 2000, **43**, 333–338.
54 G. Oberdörster, E. Oberdörster and J. Oberdörster, *Environ. Health Perspect.*, 2005, **113**, 823–839.
55 M. Geiser and W. G. Kreyling, *Part. Fibre Toxicol.*, 2010, **7**, 2.
56 H. Chen, G. Wei, A. Ispas, S. G. Hickey and A. Eychmüller, *J. Phys. Chem. C*, 2010, **114**, 21976–21981.
57 V. L. Nguyen, D. C. Nguyen, H. Hirata, M. Ohtaki, T. Hayakawa and M. Nogami, *Adv. Nat. Sci. Nanosci. Nanotechnol.*, 2010, **1**, 035012.
58 S. Sharada, P. L. Suryawanshi, R. Kumar, S. P. Gumfekar, T. B. Narsaiah and S. H. Sonawane, *Colloids Surf., A*, 2016, **498**, 297–304.
59 S. Iravani, *Green Chem.*, 2011, **13**, 2638.
60 F. J. Osonga, S. Kalra, R. M. Miller, D. Isika and O. A. Sadik, *RSC Adv.*, 2020, **10**, 5894–5904.
61 X. Yang, Q. Li, H. Wang, J. Huang, L. Lin, W. Wang, D. Sun, Y. Su, J. B. Opiyo, L. Hong, Y. Wang, N. He and L. Jia, *J. Nanoparticle Res.*, 2010, **12**, 1589–1598.
62 K. Mallikarjuna, C. Bathula, K. Buruga, N. K. Shrestha, Y.-Y. Noh and H. Kim, *Mater. Lett.*, 2017, **205**, 138–141.
63 M. Khan, G. H. Albalawi, M. R. Shaik, M. Khan, S. F. Adil, M. Kuniyil, H. Z. Alkhathlan, A. Al-Warthan and M. R. H. Siddiqui, *J. Saudi Chem. Soc.*, 2017, **21**, 450–457.
64 S. Lebaschi, M. Hekmati and H. Veisi, *J. Colloid Interface Sci.*, 2017, **485**, 223–231.
65 A. Bankar, B. Joshi, A. R. Kumar and S. Zinjarde, *Mater. Lett.*, 2010, **64**, 1951–1953.
66 R. Kumar Petla, S. Vivekanandhan, M. Misra, A. Kumar Mohanty and N. Satyanarayana, *J. Biomaterials Nanobiotechnol.*, 2012, **03**, 14–19.
67 S. Mahajan, C. K. Prashant, V. Koul, V. Choudhary and A. K. Dinda, *Curr. Nanosci.*, 2010, **6**, 413–421.
68 D. A. Ovchinnikov, *Genesis*, 2008, **46**, 447–462.
69 S. Naqvi, M. Samim, M. Z. Abdin, F. J. Ahmad, C. K. prashant and A. Dinda, *Indian J. Nephrol.*, 2010, 983.

70 L. Frenklakh, R. S. Bhat, M. Bhaskaran, S. Sharma, M. Sharma, A. Dinda and P. C. Singhal, *Dig. Dis. Sci.*, 2006, **51**, 318–325.
71 A. I. Maishi, P. K. Shoukat Ali, S. A. Chaghtai and G. Khan, *Br. Homeopath. J.*, 1998, **87**, 17–21.
72 S. Patel, *3 Biotech*, 2011, **1**, 1–9.
73 V. V. Makarov, A. J. Love, O. V. Sinitsyna, S. S. Makarova, I. V. Yaminsky, M. E. Taliansky and N. O. Kalinina, *Acta Naturae*, 2014, **6**, 35–44.
74 M. A. Noginov, G. Zhu, M. Bahoura, J. Adegoke, C. E. Small, B. A. Ritzo, V. P. Drachev and V. M. Shalaev, *Opt. Lett.*, 2006, **31**, 3022.
75 K. Tahir, S. Nazir, A. Ahmad, B. Li, S. A. Ali Shah, A. U. Khan, G. M. Khan, Q. U. Khan, Z. U. Haq Khan and F. U. Khan, *RSC Adv.*, 2016, **6**, 85903–85916.
76 R. Molaei, K. Farhadi, M. Forough and S. Hajizadeh, *J. Nanostruct.*, 2018, **8**, 47–54.
77 A. Sgambato, R. Ardito, B. Faraglia, A. Boninsegna, F. I. Wolf and A. Cittadini, *Mutat. Res. Genet. Toxicol. Environ. Mutagen*, 2001, **496**, 171–180.
78 D. Green, *Means to an End: Apoptosis and Other Cell Death Mechanisms*, Cold Spring Harbor Laboratory Press, Cold Spring Harbor, NY, 2011, ISBN 978-0-87969-888-1.
79 A. J. Kora and L. Rastogi, *Arab. J. Chem.*, 2018, **11**, 1097–1106.
80 S. Shibuya, Y. Ozawa, K. Watanabe, N. Izuo, T. Toda, K. Yokote and T. Shimizu, *PloS One*, 2014, **9**, e109288.